Dimensionality Expansion and Transfer Learning for Next Generation Energy Management Systems

Blaž Bertalanič, *Graduate Student Member, IEEE,*, Jakob Jenko and Carolina Fortuna

***Abstract*—Electrical management systems (EMS) are playing a central role in enabling energy savings. They can be deployed within an everyday household where they monitor and manage appliances and help residents be more energy efficient and subsequently also more economical. One of they key functionalities of EMS is to automatically detect and identify appliances within a household through the process of load monitoring. In this paper, we propose a new transfer learning approach for building EMS (BEMS) and study the trade-offs in terms of numbers of samples and target classes in adapting a backbone model during the transfer process. We also perform a first time analysis of feature expansion through video-like transformation of time series data for device classification in non intrusive load monitoring (NILM) and propose a deep learning architecture enabling accurate appliance identification. We examine the relative performance of our method on 5 different representative low-frequency datasets and show that our method performs with an average F1 score of 0.88 on these datasets.**

***Index Terms*—feature expansion, transfer learning, appliance classification, video-like transformation, imaging, time-series, classification, Gramian angular field, machine vision, deep learning, time series to video, load monitoring.**

I. Introduction

INCREASED energy consumption that comes with population growth and technological advances raises environmental concerns, therefore many public and private institutions are committing to emission cuts and increased energy efficiency solutions. For instance, the European Union has committed to improving energy efficiency by at least 32.5% by 2030. [1]. A promising way to achieve energy efficiency is through the use of smart power grids. These are next-generation power grids that allow bidirectional transmission of power and data, creating an automated power grid [1]. The other option is the deployment of microgrids, which is a small energy network that includes some renewable energy generation units, such as photovoltaic panels, and some households. Both smartgrids and microgrids have the flexibility to operate within the existing power grid or in island mode, providing reliable power to connected households. One of the key technologies for the successful deployment of smart grids and microgrids is the Energy Management Systems (EMS)[2], that has been shown to increase residential energy savings by more than 16% per year compared to traditional energy saving methods [3].

While Energy Management Systems have been around for about four decades, they have been evolving both conceptually and technologically [3]. For instance, some studies show that only providing information about total energy consumption does not significantly change consumers' energy consumption behavior, however, when providing finer insights, possibly into individual appliance consumption, energy saving behavior becomes noticeable [4]. As a result, future EMSs will likely include automatic monitoring and detection of household appliances capabilities able to identify individual sources of energy consumption. Such capabilities are referred to in the domain as load monitoring and can be grouped into intrusive and non-intrusive techniques [5]. Intrusive Load Monitoring (ILM) assume that each electrical device operating in a home/factory is connected to its own smart energy meter, possibly embedded in the electricity socket, that is subsequently connected to the EMS. Therefore, an ILM solution is more expensive as it requires more metering equipment, however more accurate, per device consumption data can be retrieved. For the case of Non-intrusive load monitoring (NILM), the entire energy consumption is monitored from a single central point in the home/factory where a smart meter that connects to the EMS is installed. As a result, NILM provides a cheaper solution in terms of metering equipment and infrastructure maintenance, however consumption data can only be collected in an aggregated form that need to then be processed to extract single device metering data. NILM can be seen as a two stage process in which first a dissagregation step is required followed by an ILM step that performs automatic device recognition.

For solving NILM and ILM problems, several methods have been proposed some based on combinatorics [6], thresholding [7], shallow machine learning such as Hidden Markov Models (HMM) [8], [9], [10], SVM [11], kNN [12], Naive Bayes, Logistic Regression Classifier and Decision Tree [13] and, more recently, deep learning such as recurrent neural networks (RNN)[14], [15], [16], [17], convolutional neural networks (CNN)[18], [14] or autoencoders[14], [19]. While machine learning-based solutions often yield superior appliance recognition results, only few such techniques are verified across several domain specific datasets. Additionally, especially deep learning techniques are also known to require more data for training relatively to their shallow learning counterparts, therefore it is not clear from the state of the art how much adaptation a model would require before being ready to deploy in a new EMS. To provide additional insight into the potential of deep learning techniques for appliance recognition for next generation EMS, in this paper we:

- Propose a new transfer learning (TL) approach for faster model development for building EMS (BEMS) and study the minimum number of samples needed to adapt a backbone model during the transfer process.
- Propose a new model for appliance classification developed using feature dimensionality expansion and evaluate

[1] https://ec.europa.eu/clima/eu-action/climate-strategies-targets/2030-climate-energy-framework_en

its performance on five different open source datasets. Our model uses a new representation of time series signal in video-like format based time-series to image feature expansion and a tailored deep neural network that can classify household appliances with and average F1 score of 0.88 on 5 different datasets.

This paper is organized as follows. We discuss related work in Section II. Section III provides the formal problem statement, while Section IV elaborates on various time series transformations that can be used to generate image representations. Section V introduces the proposed deep learning architecture, Section VI describes the relevant methodological and experimental details, while Section VII provides thorough analyses of the results. Finally, Section VIII concludes the paper.

II. Related work

As discussed in Section I, the purpose of using ILM or NILM in BEMS is to enable fine grained consumption tracking per appliance to stimulate energy saving behavior [3]. The community approached the fine grained consumption tracking and detail extraction using various methods from combinatorial, threshold based to machine learning to identify fronts that determine when a device is switched on and off, identify device consumption shape or forecast device usage/consumption. Nonetheless, it is in general difficult to compare different methods proposed by different researchers as they may use different datasets, pick different types of appliances to disaggregate and classify, or they use different time windows in which they try to disaggregate data or discriminate between appliances. The most frequently used datasets are UK-DALE [20], ECO [21], REDD [22], IAWE[23], REFIT [24], BLOND [25], PLAID [26] and AMPds [27], all consisting of different sets of appliance types, with either low or high-frequency sampling, which makes cross-dataset testing of trained models difficult.

A. Approaches to NILM/ILM

The first known work on the NILM problem was done by Hart [6] where different combinatorics methods to try and detect changes on the states of household appliances on aggregated signal were used. Researchers also proposed defining a set of rules or thresholds for NILM [7], but machine learning proved to be the superior method. At the beginning, the leading solutions for NILM, both disaggregation and classification/ILM, were based on Hidden Markov Models (HMM) [8], [9], [10]. HMM appears to perform well on sequential data thus are well suited method for solving NILM problems. HMM was soon outperformed by other methods of shallow machine learning like SVM [11], kNN [12], Naive Bayes, Logistic Regression Classifier and Decision Tree [13].

In the last few years deep learning became popular for solving NILM problems. Kelly *et al.* [14] were one of the first to show the suitability of deep learning for NILM. They proposed three different DL approaches, namely Long short term memory cells (LSTM), denoising autoencoders and a DL based regressor. They tried to distinguish between five different appliances in a way that they trained one network per target appliance on the raw time series data from the UK-DALE dataset, with the window width selected on an appliance-by-appliance basis varying from 13 minutes to 2.5 hours.

Other DL approaches were based on recurrent neural networks (RNN) [14], [15], [16], [17], convolutional neural networks (CNN) [18], [14] or autoencoders [14], [19]. Autoencoder based methods are mostly used for disaggregation of collected NILM data although they can also help solving the classification/ILM problem. Most of these models take raw time series data as their input.

The considered window sizes for data processing as well as the number of appliance types vary across reports and also across methods in the same report. For instance, [19], similar to [14], used different window sizes, ranging from a few minutes to up to 2 hours, depending on the 8 types of appliances considered from UK-DALE, REDD and AMPds datasets. Kim *et al.* [16] used 1 minute windows from the UK-DALE dataset and tested their approach based on Gated Recurent Unit (GRU) on classification of up to 20 different appliances. Similar to the others, Wu *et al.* [18] also used the UK-DALE dataset but tested their CNN based method also on the BLOND dataset. They took spectrogram representation of 7 second windows of raw time series as the input to their model and distinguished between 6 different appliances from the UK-DALE dataset and 6 different groups of appliances from the BLOND dataset. Le *et al.* [15] proposed their own deep learning model based on LSTM to classify whether an appliance is turned on or not. They considered five different appliances with 15 minute windowing from their own dataset.

Recently, a number of researchers have proposed to use various transfer learning (TL) techniques for NILM/ILM. In [28] it was shown that the use of a sequence-to-point DL model can be transferred between two different types of appliances, while [29] disaggregated signals using Generative Adversarial Networks and TL between houses in the same dataset. Similar research exists for appliance classification where, for example, [30] used voltage-current trajectories and showed great results in TL using pre-trained AlexNet[31] for backbone feature extraction, but their method was only tested on high frequency datasets. A similar method was shown by [32] where they proposed using recurrence plot representation (RP) of the signal and used a pre-trained VGG16 for TL. Another approach was proposed by [33] where they used their own low frequency dataset of seven appliances to train the backbone and then transferred it to unseen appliance types. In this work, the TL limitation was shown in the form of the precision drop of slightly less than 28 percentage points compared to the transfer to already known appliances.

To the best of our knowledge, this is the first attempt to study the prospect of transferring existing classification models to new houses and new EMSes that is verified across several datasets.

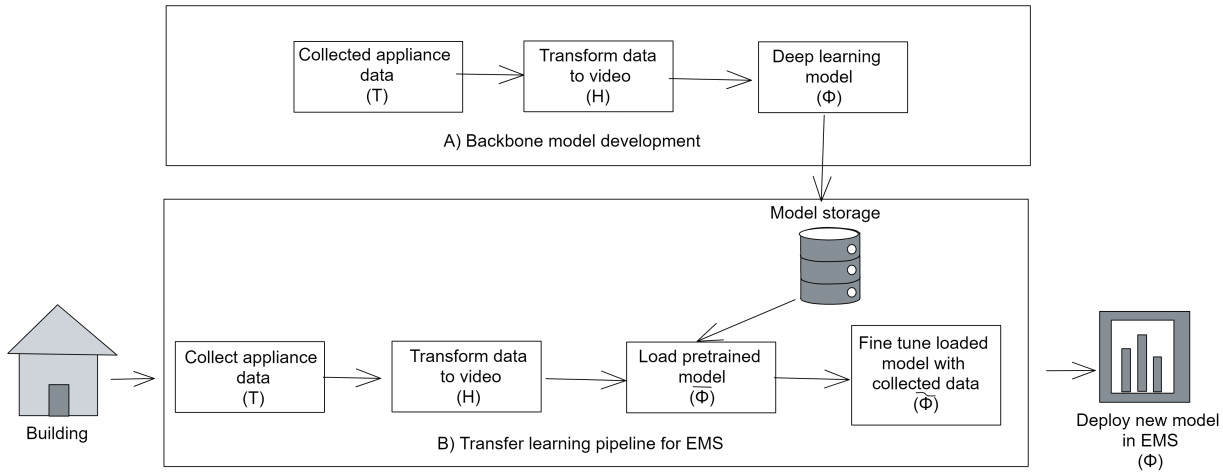

Fig. 1. Transfer learning enabled appliance classification model development for EMS.

B. Dimensionality expansion through time series to image transformation

Besides using raw time series [14], several works [34], [35] consider frequency domain or other transformations that typically preserve the dimensionality. However, more recently time-series to image transformations that expand the 1D time series into a 2D image have been considered. For instance, De Baets *et al.* [36] used the PLAID and WHITED high-frequency datasets and proposed a DL CNN model that uses a weighted pixelated image of the voltage–current trajectory (VI) as an input to classify up to 22 appliances in a few second intervals. Similar was done by [30], only on a few milliseconds interval. Later [37] used the same datasets and proposed a DL CNN model that used weighted recurrence graph plots as an input thus improving the classification performance of the model, compared to VI based approach proposed by [36].

Mottahedi *et al.* [38] were one of the first to propose using Gramian Angular Filed representation of NILM signals, where they trained three different DL models one for each appliance type, with each model using different windows between 20 and 90 minutes of time series data that was transformed into GAF. Kyrkou *et al.* [39] used the same transformation method, where they transformed 6.4min segments into GAF images and used pretrained VGG16 DL model as feature extractor and tried to detect ON/OFF state of only fridge appliance type from REDD and UK-DALE datasets. Similar thing was done by [40], where they were detecting ON/OFF state of 3 different appliance types on AMPds dataset on GAF transformation of one hour windows. Another GAF approach in combination with CNN was shown by [41], where they used their own dataset to classify 22 different appliances in a few minute windows.

We go beyond the state of the art by proposing a video-like representation of time series data by juxtaposing a series of GAF transformations totalling about 60 minute windows.

III. Problem statement

Assume a new building needs to be equipped with an EMS and connected to the smart grid as depicted on the left of Figure 1. Rather than collecting sufficient labeled data to deploy the appliance classification model in the EMS, we propose a new transfer learning (TL) approach for faster model development as depicted in the same figure. As can be seen in Figure 1 a, there is a generic appliance classification model that has been trained on a larger already collected dataset, also referred to as the backbone model. This model is saved in the model storage. As depicted in Figure 1 b, a relatively smaller number of labeled appliance data samples from the new house need to be collected and transformed to fine tune the pre-trained model loaded from the store before deploying it to the new EMS.

A. Model development

In order to populate the model storage from Figure 1 b with pre-trained models, appliance classification models need to be developed on sufficient data to achieve satisfactory performance. The required step-by-step training process is depicted in Figure 1 a and formalized in Equation 1. Given an input tensor H_i representing energy measurements from households, that has been generated from raw TS measurements T_i, there is a function Φ_i that maps the extracted features to a set of target classes C_i representing different household appliance types, where i represents one of the used datasets.

$$C_i = \Phi_i(H_i) \tag{1}$$

The classifier Φ_i is realized using one of the five different datasets to develop the deep learning model able to so solve a multi-class classification problem to discriminate between the appliance classes within the selected datasets. The cardinality of the set C_i, also denoted as $|C_i|$, denotes the number of classes to be recognized, depending on the number of appliances present in the selected dataset.

B. Model transfer

The classifier Φ_i from Equation 1 can be decomposed into two parts: a backbone function $\overline{\Phi_i}$ that extracts features from the input and a mapping function $\widetilde{\Phi_i}$ that maps those features into the target classes as per Equation 2. This decomposition enables transfering the feature generation part to a new datasets as follows.

$$\Phi_i(H_i) = \widetilde{\Phi_i}(\overline{\Phi_i}(H_i)) \tag{2}$$

Given an input of H_j, that is generated by transforming a new time series T_j, there is a function $\widetilde{\Phi_j}$, that with the process of TL uses the output from the feature extraction function $\overline{\Phi_i}$ from the function Φ_i, trained on the i-th dataset, from the input H_j, and then maps it to a set of target classes C_j as depicted in Figure 1 and can be formalized as follows:

$$C_j = \widetilde{\Phi_j}(\overline{\Phi_i}(H_j)), i \neq j \tag{3}$$

The elements of C_j can be completely different ot partially overlap with the ones of C_i and the cardinality $|C_j|$, represents the number of classes to be recognized, depending on the number of appliances in each dataset used in the TL process.

IV. Feature dimensionality expansion

We propose feature dimensionality approach using GAF transformation to realize H from Figure 1 that converts time series data into images and then juxtapose the images in a video-like format for training deep learning models. At the top of Figure 2, a windowed time series measured for an appliance is depicted across five windows. The resulting images for each windows are depicted in the lower part of the figure.

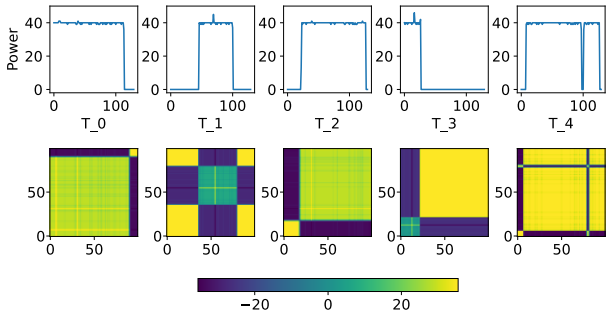

Fig. 2. Representation of each time series window and its GAF representation.

A. Gramian angular field time-series to image transformation

The Gramian angular field is an image transformation of a time series that represents the temporal correlation between points within a time series. The end result is a quadratic image representation of the input time series. This approach consists of two techniques, one is the Gramian angular summation field (GASF) and the other is the Gramian angular difference field (GADF). Both techniques are computed in a similar way, but in our work we chose to use the GASF representation because there was no difference in performance between the representations. First, the time series needs to be scaled with a min-max normalization and then transformed to a polar coordinate system. The angles ϕ_N from the polar plot are then used to calculate the GASF. The angular cosine function of the sum between two points is calculated, which is shown in Equation 4, where M represents the GASF transformation. The size of the transformed image is $N \times N$, where N represents the length of the time series used in the transformation.

$$M = \begin{pmatrix} \cos(\phi_N + \phi_1) & \cos(\phi_N + \phi_2) & \dots & \cos(\phi_N + \phi_N) \\ \vdots & \vdots & \ddots & \vdots \\ \cos(\phi_2 + \phi_1) & \cos(\phi_2 + \phi_2) & \dots & \cos(\phi_2 + \phi_N) \\ \cos(\phi_1 + \phi_1) & \cos(\phi_1 + \phi_2) & \dots & \cos(\phi_1 + \phi_N) \end{pmatrix} \tag{4}$$

B. Video-like representation

From the representation in Figure 1, it can be seen that, especially for longer time series traces, they can be split into windows of equal lengths N and each segment can then be transformed into an image M. These images can then be juxtaposed in a strict sequence as presented in Equation 5, where the tensor $H_{(NxNxR)}$ consisting of R images of size $N \times N$ can be interpreted as a video-like representation of the time series. Both size of the images M and number of juxtaposed images R are dependent on the segment length and the number of segments produced by windowing the long time series trace.

$$H_{(N \times N \times R)} = \begin{bmatrix} M_1 & M_2 & \dots & M_R \end{bmatrix} \tag{5}$$

V. Proposed classification models

In this section we first describe the proposed model transfer that solved the problem from Section III a and then elaborate on the generic model development to be made available in the model store as discussed in Section III b.

A. Proposed model

The proposed classification model, that will serve as the backbone as pe Figure 1 for our TL model, is presented in Figure 3. Considering potential resource restrictions of BEMS the backbone model was developed according to the design consideration guidelines presented in [42], making the model resource-aware. During our iteration process we considered:

- The number of convolutional layers $L_{cnn} \in \{2, 3, ...24\}$
- The number of LSTM layers $L_{lstm} \in \{1, 2, ...10\}$, with number of nodes $N_N \in \{8, 16, 24, ...128\}$

The input sequence of images is first fed into the feature extraction part of the model ($\overline{\Phi}$), that consist of convolution layer with 16 kernels of size 7×7, followed by a max pooling layer with pooling size of 2×2. Next come two similar blocks where each block consists of two convolution layers with 16 kernels of size 3×3 and max pooling layer with pooling size of 2×2. The last part of the model starts with a dropout layer of 0.1, followed by two more convolution layers with the same kernel number and size as the previous layers. All of the mentioned convolution layers use 'same' padding and stride of 1 and use use ReLU activation function, while being

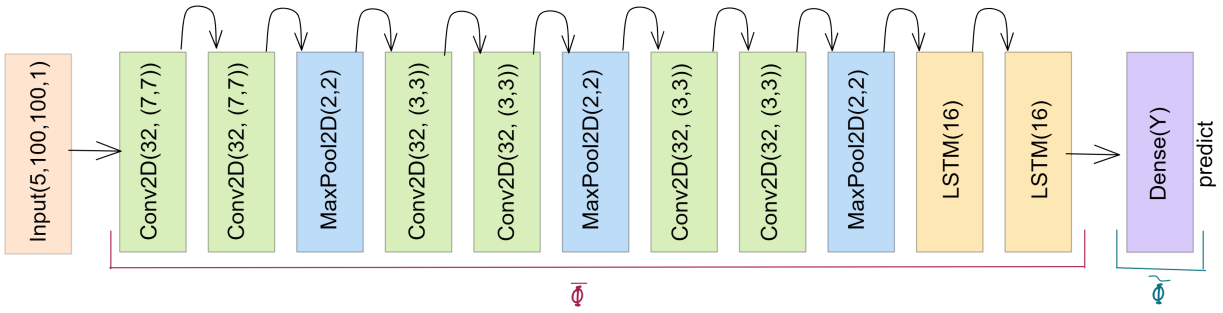

Fig. 3. Deep learning network model for NILM classification

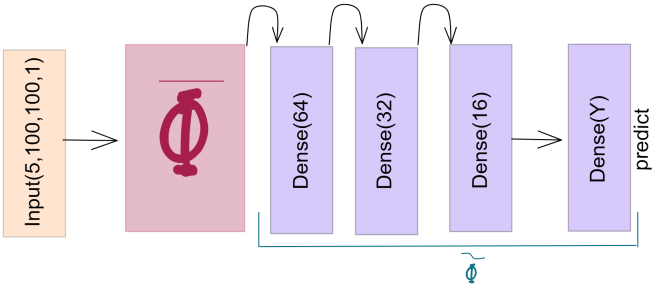

Fig. 4. Deep learning network model for TL NILM classification

embedded into the TimeDistributed class from Keras library [2]. The output data from the convolutional part of the model is then flattened and fed into two LSTM layers with 16 nodes which are also the final two layers of the feature extraction part ($\overline{\Phi}$), of the model. This output is then connected to the classification part ($\widetilde{\Phi}$), of the model consisting of only one output layer of size Y, where the softmax activation function is applied and the classification is made. The size of Y depends on the number of different classes present in the used dataset.

B. Proposed model transfer

For realizing the transfer from an existing model to a new BEMS, we propose the TL model depicted in Figure 4. The feature extraction part ($\overline{\Phi}$) is obtained from a model available in the model store as depicted in Figure 1. The backbone model is frozen and is not fine tuned during the training process. The features extracted from the backbone are fed into a classification part ($\widetilde{\Phi}$) of the model that includes three dense layers, first consisting of 64 nodes, second of 32 nodes while the third has 16 nodes. All three dense layers use the ReLU activation function. The output from the last dense layer is then fed into the final output layer of size Y, where the final classification is made after the softmax activation function is applied. The size Y depends on the number of different appliances available in the new household. The number of additional dense layers was selected based on a trial and error iterative approach. During the iterative process we considered:

- The number of additional dense layers $N_L \in \{1, 2, ...10\}$
- The number of nodes in additional dense layers $N_N \in \{8, 16, 24, ...256\}$

The final number of N_L and N_N was chosen as a performance to resource awareness trade-off.

[2]https://keras.io/api/layers/recurrent_layers/time_distributed/

VI. Methodology and Experimental Details

To present experiment details of our work we first describe the dataset generation procedure and then present details of the model training and results evaluation.

A. Dataset generation

For our experimental evaluation, we chose the UK-DALE[20], ECO [21], REDD [22], IAWE[23] and REFIT [24] dataset containing real-world measurements of power consumption. These traces were then split into smaller chunks and transformed into GASF images. For easier dataset preprocessing, the NILMTK toolkit [43] was selected as it enables easy conversion and filtering bad sectors from the data.

Table I provides a summary of the five datasets. The first column shows the dataset name, the second provides the sampling frequency used for collecting the data, while the third column shows the time period over which the samples were collected. It can be seen that all sampling rates have comparable frequency between 1 and 8 s, IAWE collection span is only 73 days while UK-DALE covers more than 4 years. To convert the TS to video-like format as discussed in Section IV-A, the data first had to be resampled to synchronize the sampling rates of the different datasets. UK-DALE was chosen with a sampling rate of 6 seconds between each sample, which resulted in a round number 10 samples per minute. Next, the data was split into sub-intervals with a fixed window length. The window length was determined based on the window that would best capture appliances operational time. Since there could still be some missing data within the subinterval due to the data collection process, a longer window length of 13 minutes was chosen, which ideally resulted in 130 samples per window. To compensate for the possible missing values in the interval, moving average was used to reduce the number of samples in the interval to 100 and also reduce noise in the data.

The forth column shows how many different houses were monitored and the fifth column gives information on how many different appliances were measured. It can be seen that

TABLE I
SUMMARY OF THE APPLIANCE MONITORING DATASETS USED IN THIS WORK.

Dataset	Sampl.	Time	Houses	Appliance	Min.	Avg.	Max.	Min. sampl.	Used
UK-DALE [20]	6s	4.3y	5	53	0	1596	15172	1986	12
ECO [21]	1s	8m	6	21	0	117	8580	236	11
REDD [22]	1s	several m[1]	6	17	0	88	582	275	4
IAWE [23]	1s	73d	1	9	0	183	747	81	4
REFIT [24]	8s	2y	20	23	71	12873	72600	289	15

[1] Authors claim they collected the data through several months but did not provide an exact number

IAWE only contains data from one house with 9 appliances, UK-DALE contains 5 houses and 53 appliances while REFIT includes 20 houses and 23 appliances. Columns 6-8 provide the minimum, average and maximum samples that can be extracted for each device using the selected 13 minute window. It can be seen that in all datasets but REFIT, there are devices for which no training example can be generated while the maximum number of samples differ by orders of magnitude, from hundreds in REDD and IAWE to tens of thousands in UK-DALE and REFIT. After the cleaning and windowing, the GASF transformation was applied resulting in images of size 100×100 pixels that subsequently need to be juxtaposed in strict order. We selected to juxtapose 5 GASF images in strict time order, ultimately representing a 62 minute or approximately one hour operating window for each device. An example representation of one sample of fridge/freezer from UK-DALE dataset can be seen in the Figure2. In the upper row of the figure we see a sequence of time series data for 62 minutes in succession from left to right. In the bottom row there are image transformations corresponding to each sub-interval above it.

Finally the last column shows the number of appliance classes used in the final dataset after preprocessing and transformation, where certain appliance types were discarded due to low sample size (i.e. missing data). Based on empirical test presented later in Section VII, we excluded all appliance types that had less than 230 samples. By using domain knowledge, we also decided to treat appliances like fridge and freezer as the same type of device, since in its core they operate in the same way. Similar was done for toaster and kettle, since both devices use a similar heating element only the function of what is being heated is different, creating a new appliance type named heating element kitchen appliances (HEKA). This process resulted in only using 12 out of the available 53 appliances in UK-DALE, 11 out of 21 for ECO, 4 out of 17 for REDD, and 15 out of 23 for REFIT. Since IAWE is a small dataset, we allowed 81 samples for this case which led to keeping 4 out of 9 appliances.

B. Model training and evaluation

For training, we shuffled each dataset and split it into a training and a test dataset in an 80:20 ratio. We performed the shuffle split three times and then trained the model on the training set and evaluated it on the test set of each dataset used separately. The results presented are averages of all shuffle split metrics results. Due to the imbalance of the datasets, we weighted the classes during the training process. The goal is to penalize misclassification by the minority classes by setting a higher class weight while reducing the weight for the majority class. The weights were assigned inversely proportional to the proportion of the class in the dataset, i.e., the classes with the lowest proportion were assigned the highest weight and those with the highest proportion were assigned the lowest weight. The backbone models were trained for 150 epochs and batch size 32, while the TL model was trained for 50 epochs with the same batch size.

For performance evaluation we use the standard metrics precision, recall and F1 score for each class. The precision measures how many detected instances of a certain class actually belong to that class, expressed as: Precision = $\frac{TP}{TP+FP}$, while recall measures how many of the instances belonging to a certain class were actually detected and is expressed as: Recall = $\frac{TP}{TP+FN}$, where TP, FP and FN stand for true positives, false positives and false negatives. With precision and recall we can calculate the harmonic mean between the two and get the F1 score, where larger values indicate better classifier.

C. Baseline model

To compare how the proposed model fairs against other dimensionality expansion models a baseline model was developed. Each dataset was sliced into 60 minute long windows and each window was then transformed into GASF image. Since the average 60 minute sample of time series transformed into images contains up to 600 samples, a direct transformation would produce larger images of size 600×600 pixels, which require substantially more computational power to train. To keep the size of the output images within reasonable limits, a rolling averaging process is applied to the time series that reduces its size to 300 samples, which are then converted to images of size 300×300 pixels.

A series of well know DL architectures were tried and the one with the best performance results was selected. AlexNet [31] and VGG11 to VGG16 [44] were all tested, due to their similarity to our model, and in the end VGG11 performed the best out of all the tested architectures and was selected as baseline model.

D. Determining the number of classes and samples needed for transfer learning

To analyze how the number of classes in a dataset used for training a backbone model affects the TL process, a multitude

of backbone models were trained, each with a different number of classes present in the subset of training dataset. Since REFIT dataset has the highest number of different classes this was used as the main dataset for generating the subset training datasets. For each subset, the classes were selected at random. The first subset contained two different classes and then, with each iteration, we increased the number of randomly selected appliance types by one until all of the 15 classes was used. Each trained backbone model was then used in the architecture presented in Section V a and tested on the subset of ECO dataset for faster testing. For each iteration an average F1 was recorded.

We also analyzed how the number of positive samples of each class affects the backbone training process. Twelve experiments were conducted, where the number of samples for each class was increasing from 50 to 550 samples with a step of 50. Each backbone model was trained using the architecture presented in Section V a and tested according to methodology presented in Section VI b and an average F1 score was recorded. We were mostly interested in the smallest number of samples needed to train a useful backbone model.

For plotting the results and approximating the recorded discrete values, the Savitzky–Golay filter was used with 1st order polynomials and window length of 3.

VII. Results

In this section, we evaluate the relative performance of the proposed feature expansion approach proposed in Section IV and designed model proposed in Section V for solving the NILM general classification problem formulated in Section III. The experimental details used to obtain the results are detailed in SectionVI.

A. Evaluating the backbone model

The results for each dataset are presented in Tables II–VI. For these five table, the first column lists the classes (C_i), while the remaining three columns list the selected metrics. The last row of each table is reserved for the weighted averages of the selected metrics, that compensates for the unbalanced representation of classes and thus enables easier comparison between the results of different methods and datasets. From the results listed in Tables II–VI, three high level observations are outlined as follows.

- In terms of F1 score, our proposed method outperforms the baseline in three out of the five datasets, while for the remaining two, the performance is only slightly below the baseline.
- The difference in the F1 score performance between the proposed model and the baseline increases with the number of classes in the dataset.
- In general, the detection of devices with short duration patterns, such as microwave and HEKA, is improved with our method compared to the baseline.

From Table II, it can be seen that the proposed model performs with an F1 score starting from 0.90 for most of the classes selected in UK-DALE. In terms of F1 score, our proposed method outperforms the baseline VGG11 method by up to 0.18, except HEKA and microwaves. According to the weighted average of the F1 score, our method overall outperforms the VGG11 by 0.06. Since the computer monitor and desktop computers have a similar pattern and can be easily confused by the models, it can be seen from the table that our method significantly improves upon the results of the baseline model with a difference in F1 score of up to 0.18.

TABLE II
UKDALE CLASSIFICATION RESULTS

Class	Proposed model			baseline VGG11		
	Prec.	Rec.	F1	Prec.	Rec.	F1
HEKA	0.95	0.87	0.90	0.89	0.93	0.91
fridge/freezer	0.99	0.97	0.98	0.96	0.97	0.96
HTPC	0.93	0.95	0.94	0.75	0.80	0.77
boiler	0.97	0.97	0.97	0.92	0.91	0.91
computer monitor	0.88	0.93	0.90	0.72	0.72	0.72
desktop computer	0.92	0.96	0.94	0.80	0.75	0.77
laptop computer	0.99	0.97	0.98	0.91	0.91	0.91
light	0.97	0.98	0.98	0.90	0.84	0.87
microwave	0.78	0.90	0.84	0.88	0.89	0.89
server computer	0.98	0.96	0.97	0.95	0.95	0.95
television	0.96	0.90	0.93	0.82	0.81	0.81
washer dryer	0.97	0.99	0.98	0.93	0.91	0.92
Weighted avg.	0.94	0.94	0.94	0.88	0.88	0.88

TABLE III
ECO CLASSIFICATION RESULTS

Class	Proposed model			baseline VGG11		
	Prec.	Rec.	F1	Prec.	Rec.	F1
HEKA	0.99	0.98	0.99	0.93	0.97	0.95
fridge/freezer	0.99	0.95	0.97	0.99	0.98	0.98
HTPC	0.89	0.72	0.79	0.89	0.81	0.85
audio system	0.58	0.85	0.69	0.68	0.81	0.74
broadband router	0.97	0.99	0.98	0.65	0.34	0.66
coffee maker	0.86	1.00	0.92	0.93	0.91	0.92
computer	0.92	0.93	0.92	0.94	0.95	0.95
lamp	0.54	0.87	0.67	0.83	0.87	0.85
laptop computer	0.74	0.90	0.81	0.79	0.88	0.83
microwave	0.98	0.98	0.98	0.66	0.82	0.73
washing machine	1.00	0.94	0.97	0.81	0.86	0.83
Weighted avg.	0.92	0.90	0.91	0.94	0.94	0.94

It can be seen from the last row of Table III that in terms of weighted average F1 score, our method is slightly worse compared to the VGG11 baseline model. Although the baseline model outperforms our model for five out of eleven classes, the performance difference is not significant, with the exception of the lamp class. For the lamp class, our model performs with an F1 score of 0.67 compared to 0.85 for the baseline model. At the same time, we can see that our model significantly outperforms the baseline in detecting the microwave class with and F1 score greater by 0.25 and broadband router class that has an F1 score greater by 0.32 which might indicate a superior ability to detect appliances with a short working cycle.

TABLE IV
REDD CLASSIFICATION RESULTS

Class	Proposed model			baseline VGG11		
	Prec.	Rec.	F1	Prec.	Rec.	F1
fridge/freezer	0.76	0.92	0.83	0.89	0.93	0.91
electric furnace	0.77	0.86	0.81	0.85	0.92	0.88
light	0.82	0.72	0.77	0.81	0.80	0.81
microwave	0.78	0.95	0.85	0.49	0.71	0.58
sockets	0.75	0.72	0.74	0.81	0.73	0.76
Weighted avg.	0.78	0.78	0.78	0.82	0.81	0.81

The performance of the model on the REDD dataset, that is smaller than the previous two, can be found in Table IV. In terms of the weighted average F1 score, the baseline model slightly outperforms our proposed model by 0.03. Similar to the ECO dataset, the proposed model is not significantly worse at detecting appliances, with the exception of the microwave class where it considerably outperforms the baseline model. The model detects the microwave class with an F1 score of 0.85 which is by 0.27 better than the baseline model. This is consistent with our observation that appliances with short working duration are in general easier to detect with our proposed method compared to the baseline.

TABLE V
IAWE CLASSIFICATION RESULTS

Class	Proposed model			baseline VGG11		
	Prec.	Rec.	F1	Prec.	Rec.	F1
air conditioner	1.00	1.00	1.00	1.0	0.87	0.93
computer	0.99	0.98	0.98	0.95	0.96	0.95
fridge/freezer	0.98	0.98	0.98	0.96	0.96	0.96
television	0.78	0.88	0.82	0.78	0.88	0.82
Weighted avg.	0.98	0.97	0.97	0.95	0.95	0.95

The performance results for the IAWE, the smallest dataset, reflected in Table V, show superior performance compared to the other datasets. According to the weighted average F1 score, our proposed method slightly outperforms the baseline model by 0.02, being better at detecting three out of four classes, and achieving the same F1 score as the baseline model in the detection of the television class.

The evaluation results for REFIT, the largest dataset, are shown in Table VI. Compared to the baseline, our proposed model significantly outperform it by 0.12 according to the weighted averaged F1. Considering also the results in Table II, a trend can be observed that our proposed method starts outperforming the baseline when the number of classes in the dataset increases, therefore having superior discrimination power. In terms of F1 score, our proposed method outperforms the baseline for every class of this dataset. An additional observation is that in most cases recall is much higher then precision for the proposed model, that can be explained by the unbalanced nature of the dataset and is subsequently taken into account by the weighted average scores, where we can see that precision slightly outperforms the recall.

TABLE VI
REFIT CLASSIFICATION RESULTS

Class	Proposed model			baseline VGG11		
	Prec.	Rec.	F1	Prec.	Rec.	F1
HEKA	1.00	0.99	1.00	0.89	0.86	0.87
fridge/freezer	0.98	0.97	0.97	0.91	0.92	0.91
audio system	0.40	0.89	0.55	0.38	0.43	0.40
bread maker	0.90	1.00	0.95	0.62	0.72	0.66
broadband router	0.44	0.87	0.58	0.41	0.45	0.43
computer	0.87	0.81	0.84	0.64	0.58	0.61
dehumidifier	0.66	0.95	0.78	0.74	0.69	0.71
dish washer	0.96	0.98	0.97	0.86	0.86	0.86
electric space heater	0.71	0.88	0.78	0.61	0.60	0.60
food processor	0.77	0.95	0.85	0.70	0.65	0.68
pond pump	0.78	0.99	0.87	0.72	0.82	0.77
television	0.91	0.82	0.86	0.75	0.76	0.75
tumble dryer	0.87	0.84	0.86	0.68	0.70	0.69
washer dryer	0.69	0.59	0.64	0.30	0.34	0.32
washing machine	0.88	0.91	0.89	0.83	0.82	0.83
Weighted avg.	0.92	0.91	0.91	0.80	0.79	0.79

When we analyze the results of all datasets, we can see that our proposed method mainly improves the detection of appliances with short working duration such as microwave, HEKA, and others. The reason is that the baseline images are larger than those used in the video-like format. This degrades the resolution of the patterns, which can cause short power spikes to be easily missed by the VGG11 model. The other reason is due to the implementation of the transformations of time series into images for the baseline VGG11 model. Since, according to SectionVI c, a direct transformation would produce larger images than the VGG11 model can sustainably handle so a rolling averaging process is applied to the TS before transformation, but the trade-off is a partial loss of information within the TS. Compared to the conventional conversion of time series into images, our method helps to improve the resolution of the patterns in transformed TS and also helps reduce the information loss that may occur when converting time series into images.

B. Analysis of samples needed for successful backbone training process

Figure 5 presents the effect of the number of samples on backbone training process. It can be seen from the graph that the average F1 score steadily rises with the increase of the number of samples. The elbow of the curve shows at around 150 samples where the F1 score is around 0.70. Performing and evaluating the transfer learning, we selected the minimum number of samples per class at 230 aiming for an F1 score around 0.75.

C. Analysis of classes used in the backbone model on the success of transfer learning

In Figure 6 the effect that the number of different classes have on TL is presented. The elbow curve occurs between 5 and 6 classes which results in an average F1 score between

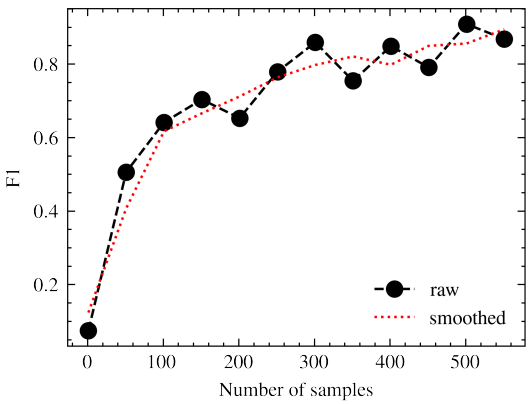

Fig. 5. Effect of selected number of samples in the dataset on the average F1 score of TL

0.70 and 0.75. What can also be observed is that the average F1 score steadily increases with the number of different devices present in the dataset. This shows that with the increase in diversity and number of devices, the trained model can extract more general features from the data which can then be easier applied to unseen cases in other datasets.

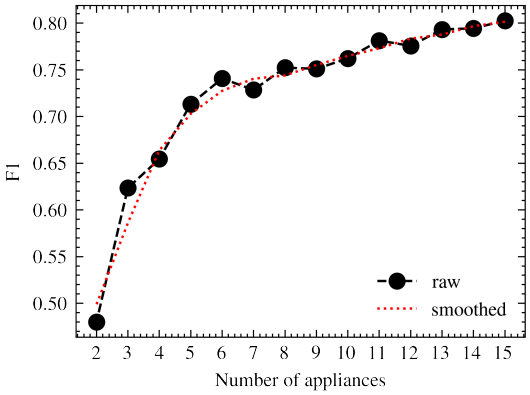

Fig. 6. Effect of selected number of appliances in the backbone model on the average F1 score of TL

D. Evaluating the transfer learning model

In this section, we evaluate the relative performance of the TL deep learning model proposed in Section V for solving the NILM TL classification problem formulated in Section III. The experimental details used to obtain the results are detailed in SectionVI. According to the experimental results in Section VII-C, which shows how important the number of different classes is for the classification performance of a model, the model trained on REFIT was chosen for the backbone of our TL model because it had the highest number of classes used in training, while it performed with a similar F1 score as the models trained on UK-DALE and ECO.

Table VII shows the results of the TL classifier for the UK-DALE, ECO, REDD, and IAWE datasets. The first column of the table lists the datasets, second column of the table represents classes, and the remaining three columns list the selected performance metrics. The first thirteen rows of the table show the results of the UK-DALE classifier, the next twelve rows belong to the ECO dataset, followed by six rows showing the results of REDD, and finally the last five rows represent the results for IAWE. From the results listed the table, three high level observations are outlined as follows.

- According to the weighted F1 score, the overall performance drop compared to traditional training method varies between 0.02 for IAWE and 0.16 for ECO.
- In general, devices that also perform well on REFIT while training the backbone model, such as HEKA, fridge/freezer and computer, show better performance in term of F1 score compared to those appliances that are not present.
- Due to the unbalanced nature of the dataset, the recall is in general higher than precision, similar to results in the previous subsection.

The first twelve rows of the Table VII show the results of transferring the backbone model to UK-DALE. In general, it is evident that the model performs with a weighted F1 score of 0.85, which is by 0.09 worse than the model trained from scratch in Table II. Compared to Table II, the highest performance drop in terms of F1 score can be observed for the desktop computer and light classes, both of them dropping their F1 score by 0.14, while the laptop computer and washer dryer classes are performing worse by only 0.04.

The next eleven rows of the Table VII, show the results of the transferred ECO classifier. According to the weighted F1 score, ECO performs worse by 0.16 compared to the ECO model trained from scratch. Here the worst F1 score can be observed for the broadband router, 0.40, and washing machine class with an F1 drop of 0.41. The best performing class is HEKA which performs with only 0.01 worse F1 score compared to the results in Table III.

The TL model performance for the REDD dataset can be found in the next six rows under the ECO dataset results in Table VII. In general, the performance of the TL model in terms of weighted F1 score is 0.04 worse than that of the model trained from scratch. The model performs best in detecting the microwave class with an F1 score of 0.87 which is by 0.02 better then the model trained from scratch in Table IV. The highest drop, compared to the F1 score in Table IV, can be seen for the electric furnace class which is worse by 0.10. All the remaining classes also perform worse, but their F1 score drop ranges between 0.02 for light and 0.05 for the fridge/freezer class.

The remaining five rows refer to the IAWE dataset TL model performance results as listed in Table VII. The general observation is that the TL model again achieves the highest weighted average F1 results among all the selected datasets. The model achieves a weighted average F1 score of 0.95, which is 0.02 lower than the model trained from scratch in Table V. The model is able to classify the air conditioner class with a perfect F1 score of 1.00 which is the same as for the model trained from scratch. In terms of F1 score, both the computer and fridge/freezer classes perform slightly worse than in Table V with the drop being 0.01 and 0.03, respectively.

TABLE VII
TL RESULTS ON SELECTED DATASETS

Dataset	Class	Refit backbone model		
		Prec.	Rec.	F1
UK-DALE	HEKA	0.88	0.78	0.83
	fridge/freezer	0.94	0.92	0.93
	HTPC	0.77	0.81	0.79
	boiler	0.88	0.89	0.89
	computer monitor	0.81	0.75	0.77
	desktop computer	0.77	0.84	0.80
	laptop computer	0.98	0.90	0.94
	light	0.79	0.90	0.84
	microwave	0.66	0.80	0.72
	server computer	0.80	0.93	0.86
	television	0.88	0.84	0.86
	washer dryer	0.95	0.93	0.94
	Weighted avg.	0.85	0.85	0.85
ECO	HEKA	0.99	0.97	0.98
	fridge/freezer	0.98	0.78	0.87
	HTPC	0.71	0.46	0.56
	audio system	0.52	0.74	0.61
	broadband router	0.45	0.85	0.58
	coffee maker	0.57	0.94	0.71
	computer	0.84	0.71	0.77
	lamp	0.22	0.65	0.32
	laptop computer	0.53	0.73	0.62
	microwave	0.78	0.97	0.87
	washing machine	0.39	0.96	0.56
	Weighted avg.	0.82	0.73	0.75
REDD	fridge/freezer	0.68	0.91	0.78
	electric furnace	0.61	0.86	0.71
	light	0.79	0.71	0.75
	microwave	0.81	0.95	0.87
	sockets	0.78	0.64	0.70
	Weighted avg.	0.75	0.74	0.74
IAWE	air conditioner	1.00	1.00	1.00
	computer	0.99	0.96	0.97
	fridge/freezer	0.98	0.92	0.95
	television	0.50	0.94	0.65
	Weighted avg.	0.96	0.94	0.95

The classification of the television class is the worst with an F1 score of 0.65, which is by 0.17 worse than in Table V.

The results show that training a feature extraction model can help simplify model development for the BEMS system with the process of transfer learning. Although all four datasets experienced a performance drop compared to the models trained from scratch, the performance was still within acceptable range especially considering it takes 3 times less epochs to train such model. [33] reported in their paper a drop in precision of about 28 percentage points when transferring the model to unseen device types. In our case, four out of five classes in the dataset REDD are not part of the dataset REFIT and the precision drop for these classes was up to 16 percentage points, so compared to [33], our precision drop is up to 12 percentage points lower.

VIII. Conclusion

In this paper, we performed a first time analysis of video-like representation of time series for NILM appliance classification and proposed a new deep neural network architecture that is able to distinguish between different devices. We tested our proposed method on five different datasets and showed an average F1 score of 0.88. We also analyse the usability of our proposed method in transfer learning cross-dataset training with an average weighted F1 score of 0.80, which is only 0.08 worse compared to training the model from scratch. We also provided insight into how the number of training samples and the number of different classes impact the transfer learning model training. We show that using our model you need at least 230 samples to train a good enough classifier with an average F1 score of 0.75, while we also show that the more classes are present while training the feature extraction model, the better the performance of transfer learning.

References

[1] X. Fang, S. Misra, G. Xue, and D. Yang, "Smart grid — the new and improved power grid: A survey," *IEEE Communications Surveys Tutorials*, vol. 14, no. 4, pp. 944–980, 2012.

[2] M. Zhuang, M. Shahidehpour, and Z. Li, "An overview of non-intrusive load monitoring: Approaches, business applications, and challenges," in *2018 International Conference on Power System Technology (POWERCON)*, 2018, pp. 4291–4299.

[3] D. Lee and C.-C. Cheng, "Energy savings by energy management systems: A review," *Renewable and Sustainable Energy Reviews*, vol. 56, pp. 760–777, 2016. [Online]. Available: https://www.sciencedirect.com/science/article/pii/S1364032115013349

[4] M. Hazas, A. Friday, and J. Scott, "Look back before leaping forward: Four decades of domestic energy inquiry," *IEEE pervasive Computing*, vol. 10, no. 1, pp. 13–19, 2010.

[5] E. Gomes and L. Pereira, "Pb-nilm: Pinball guided deep non-intrusive load monitoring," *IEEE Access*, vol. 8, pp. 48 386–48 398, 2020.

[6] G. Hart, "Nonintrusive appliance load monitoring," *Proceedings of the IEEE*, vol. 80, no. 12, pp. 1870–1891, 1992.

[7] P. Bilski and W. Winiecki, "The rule-based method for the non-intrusive electrical appliances identification," in *2015 IEEE 8th International Conference on Intelligent Data Acquisition and Advanced Computing Systems: Technology and Applications (IDAACS)*, vol. 1. IEEE, 2015, pp. 220–225.

[8] M. Aiad and P. H. Lee, "Non-intrusive load disaggregation with adaptive estimations of devices main power effects and two-way interactions," *Energy and Buildings*, vol. 130, pp. 131–139, 2016.

[9] O. Parson, S. Ghosh, M. Weal, and A. Rogers, "Non-intrusive load monitoring using prior models of general appliance types," in *Twenty-Sixth AAAI Conference on Artificial Intelligence*, 2012.

[10] F. Paradiso, F. Paganelli, D. Giuli, and S. Capobianco, "Context-based energy disaggregation in smart homes," *Future Internet*, vol. 8, no. 1, 2016. [Online]. Available: https://www.mdpi.com/1999-5903/8/1/4

[11] Y.-X. Lai, C.-F. Lai, Y.-M. Huang, and H.-C. Chao, "Multi-appliance recognition system with hybrid svm/gmm classifier in ubiquitous smart home," *Information Sciences*, vol. 230, pp. 39–55, 2013.

[12] D. Weiβhaar, P. Held, S. Mauch, and D. Benyoucef, "Device classification for nilm using fit-ps compared with standard signal forms," in *2018 International IEEE Conference and Workshop in Óbuda on Electrical and Power Engineering (CANDO-EPE)*. IEEE, 2018, pp. 1–6.

[13] J. Gao, E. C. Kara, S. Giri, and M. Berges, "A feasibility study of automated plug-load identification from high-frequency measurements," in *2015 IEEE global conference on signal and information processing (GlobalSIP)*. IEEE, 2015, pp. 220–224.

[14] J. Kelly and W. Knottenbelt, "Neural nilm: Deep neural networks applied to energy disaggregation," ser. BuildSys '15. New York, NY, USA: Association for Computing Machinery, 2015, p. 55–64. [Online]. Available: https://doi.org/10.1145/2821650.2821672

[15] T.-T.-H. Le and H. Kim, "Non-intrusive load monitoring based on novel transient signal in household appliances with low sampling rate," *Energies*, vol. 11, no. 12, 2018. [Online]. Available: https://www.mdpi.com/1996-1073/11/12/3409

[16] J. Kim, H. Kim *et al.*, "Classification performance using gated recurrent unit recurrent neural network on energy disaggregation," in *2016 international conference on machine learning and cybernetics (ICMLC)*, vol. 1. IEEE, 2016, pp. 105–110.

[17] O. Krystalakos, C. Nalmpantis, and D. Vrakas, "Sliding window approach for online energy disaggregation using artificial neural networks," in *Proceedings of the 10th Hellenic Conference on Artificial Intelligence*, ser. SETN '18. New York, NY, USA: Association for Computing Machinery, 2018. [Online]. Available: https://doi.org/10.1145/3200947.3201011

[18] Q. Wu and F. Wang, "Concatenate convolutional neural networks for non-intrusive load monitoring across complex background," *Energies*, vol. 12, no. 8, 2019. [Online]. Available: https://www.mdpi.com/1996-1073/12/8/1572

[19] R. Bonfigli, A. Felicetti, E. Principi, M. Fagiani, S. Squartini, and F. Piazza, "Denoising autoencoders for non-intrusive load monitoring: Improvements and comparative evaluation," *Energy and Buildings*, vol. 158, pp. 1461–1474, 2018. [Online]. Available: https://www.sciencedirect.com/science/article/pii/S0378778817314457

[20] J. Kelly and W. Knottenbelt, "The UK-DALE dataset, domestic appliance-level electricity demand and whole-house demand from five UK homes," *Scientific Data*, vol. 2, no. 150007, 2015.

[21] C. Beckel, W. Kleiminger, R. Cicchetti, T. Staake, and S. Santini, "The eco data set and the performance of non-intrusive load monitoring algorithms," in *Proceedings of the 1st ACM conference on embedded systems for energy-efficient buildings*, 2014, pp. 80–89.

[22] J. Z. Kolter and M. J. Johnson, "Redd: A public data set for energy disaggregation research," in *Workshop on data mining applications in sustainability (SIGKDD), San Diego, CA*, vol. 25, no. Citeseer, 2011, pp. 59–62.

[23] N. Batra, M. Gulati, A. Singh, and M. B. Srivastava, "It's different: Insights into home energy consumption in india," in *Proceedings of the 5th ACM Workshop on Embedded Systems For Energy-Efficient Buildings*, 2013, pp. 1–8.

[24] D. Murray, L. Stankovic, and V. Stankovic, "An electrical load measurements dataset of united kingdom households from a two-year longitudinal study," *Scientific data*, vol. 4, no. 1, pp. 1–12, 2017.

[25] T. Kriechbaumer and H.-A. Jacobsen, "Blond, a building-level office environment dataset of typical electrical appliances," *Scientific data*, vol. 5, no. 1, pp. 1–14, 2018.

[26] J. Gao, S. Giri, E. C. Kara, and M. Berges, "Plaid: A public dataset of high-resoultion electrical appliance measurements for load identification research: Demo abstract," in *Proceedings of the 1st ACM Conference on Embedded Systems for Energy-Efficient Buildings*, ser. BuildSys '14. New York, NY, USA: Association for Computing Machinery, 2014, p. 198–199. [Online]. Available: https://doi.org/10.1145/2674061.2675032

[27] S. Makonin, F. Popowich, L. Bartram, B. Gill, and I. V. Bajić, "Ampds: A public dataset for load disaggregation and eco-feedback research," in *2013 IEEE electrical power & energy conference*. IEEE, 2013, pp. 1–6.

[28] M. D'Incecco, S. Squartini, and M. Zhong, "Transfer learning for non-intrusive load monitoring," *IEEE Transactions on Smart Grid*, vol. 11, no. 2, pp. 1419–1429, 2020.

[29] A. M. A. Ahmed, Y. Zhang, and F. Eliassen, "Generative adversarial networks and transfer learning for non-intrusive load monitoring in smart grids," in *2020 IEEE International Conference on Communications, Control, and Computing Technologies for Smart Grids (SmartGridComm)*, 2020, pp. 1–7.

[30] Y. Liu, X. Wang, and W. You, "Non-intrusive load monitoring by voltage–current trajectory enabled transfer learning," *IEEE Transactions on Smart Grid*, vol. 10, no. 5, pp. 5609–5619, 2019.

[31] A. Krizhevsky, I. Sutskever, and G. E. Hinton, "Imagenet classification with deep convolutional neural networks," *Advances in neural information processing systems*, vol. 25, pp. 1097–1105, 2012.

[32] D. L. Cavalca and R. A. S. Fernandes, "Deep transfer learning-based feature extraction: An approach to improve nonintrusive load monitoring," *IEEE Access*, vol. 9, pp. 139 328–139 335, 2021.

[33] Z. Zhou, Y. Xiang, H. Xu, Z. Yi, D. Shi, and Z. Wang, "A novel transfer learning-based intelligent nonintrusive load-monitoring with limited measurements," *IEEE Transactions on Instrumentation and Measurement*, vol. 70, pp. 1–8, 2021.

[34] P. Held, S. Mauch, A. Saleh, D. Ould Abdeslam, and D. Benyoucef, "Frequency invariant transformation of periodic signals (fit-ps) for classification in nilm," *IEEE Transactions on Smart Grid*, vol. 10, no. 5, pp. 5556–5563, 2019.

[35] Y.-C. Su, K.-L. Lian, and H.-H. Chang, "Feature selection of non-intrusive load monitoring system using stft and wavelet transform," in *2011 IEEE 8th International Conference on e-Business Engineering*, 2011, pp. 293–298.

[36] L. De Baets, J. Ruyssinck, C. Develder, T. Dhaene, and D. Deschrijver, "Appliance classification using vi trajectories and convolutional neural networks," *Energy and Buildings*, vol. 158, pp. 32–36, 2018. [Online]. Available: https://www.sciencedirect.com/science/article/pii/S0378778817312690

[37] A. Faustine and L. Pereira, "Improved appliance classification in non-intrusive load monitoring using weighted recurrence graph and convolutional neural networks," *Energies*, vol. 13, no. 13, 2020. [Online]. Available: https://www.mdpi.com/1996-1073/13/13/3374

[38] M. Mottahedi and S. Asadi, "Non-intrusive load monitoring using imaging time series and convolutional neural networks," in *16th International Conference on computing in civil and building engineering*, 2016, pp. 705–710.

[39] L. Kyrkou, C. Nalmpantis, and D. Vrakas, "Imaging time-series for nilm," in *International Conference on Engineering Applications of Neural Networks*. Springer, 2019, pp. 188–196.

[40] S. R. Tito, A. Ur Rehman, Y. Kim, P. Nieuwoudt, S. Aslam, S. Soltic, T. T. Lie, N. Pandey, and M. D. Ahmed, "Image segmentation-based event detection for non-intrusive load monitoring using gramian angular summation field," in *2021 IEEE Industrial Electronics and Applications Conference (IEACon)*, 2021, pp. 185–190.

[41] D. Jia, X. Huang, Z. Du, R. Li, and K. Li, "Identification of electrical equipment based on two-dimensional time series characteristics of power," in *IOP Conference Series: Materials Science and Engineering*, vol. 768, no. 6. IOP Publishing, 2020, p. 062019.

[42] B. Bertalanič, M. Meža, and C. Fortuna, "Resource-aware time series imaging classification for wireless link layer anomalies," *IEEE Transactions on Neural Networks and Learning Systems*, pp. 1–13, 2022.

[43] N. Batra, J. Kelly, O. Parson, H. Dutta, W. Knottenbelt, A. Rogers, A. Singh, and M. Srivastava, "Nilmtk: An open source toolkit for non-intrusive load monitoring," in *Proceedings of the 5th International Conference on Future Energy Systems*, ser. e-Energy '14. New York, NY, USA: Association for Computing Machinery, 2014, p. 265–276. [Online]. Available: https://doi.org/10.1145/2602044.2602051

[44] K. Simonyan and A. Zisserman, "Very deep convolutional networks for large-scale image recognition," *arXiv preprint arXiv:1409.1556*, 2014.